LABORATORY OF
CONSTRUCTION
MATERIALS

DISSOLUTION THEORY APPLIED TO THE INDUCTION PERIOD IN ALITE HYDRATION

Patrick Juilland
Aditya Kumar
Dr. Emmanuel Gallucci
Dr. Robert J. Flatt
Prof. Karen Scrivener

Outline

- General mechanisms about the hydration of cementitious materials
- Description of the different existing theories about the induction period
- Discussion from the point of view of geochemistry
- Results from this work
- Proposed mechanism for the early hydration of alite in paste
- Conclusions

Calorimetry and solution composition

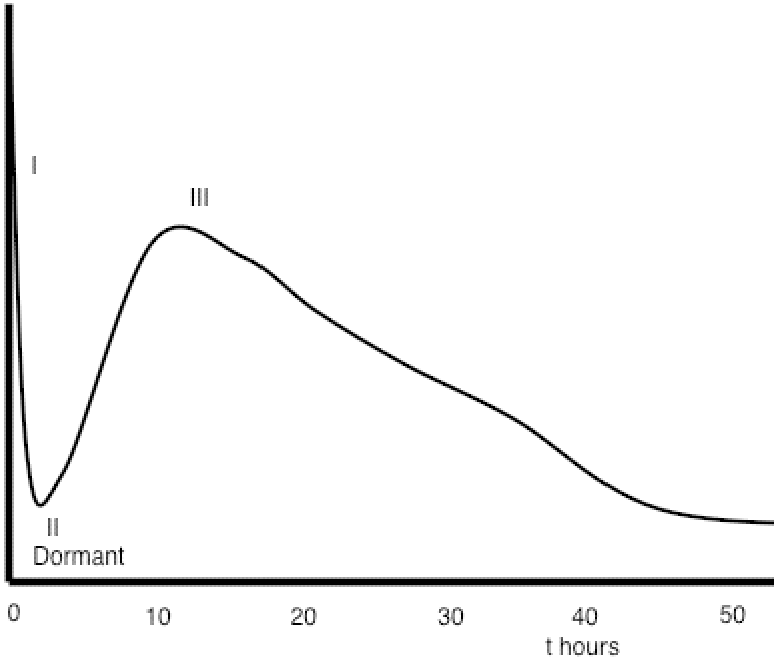

Typical calorimetry curve for the hydration of cement

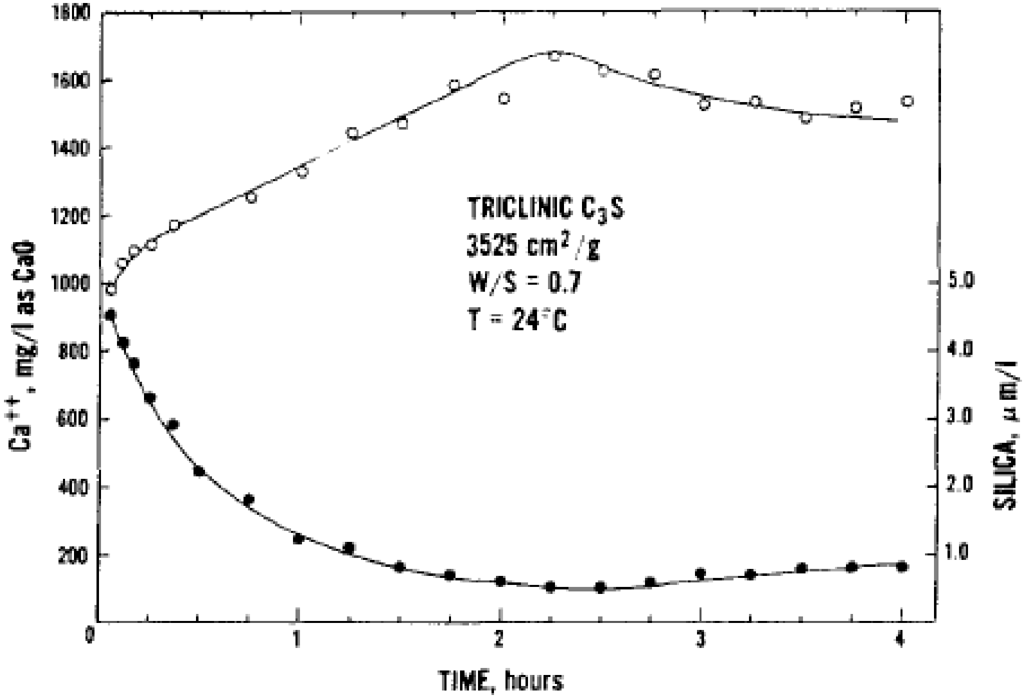

Calcium ion and silica concentrations in solution during the first 4 hours of hydration at a w/C_3S ratio of 0.7.
[Brown et al. 1984]

Different theories about the induction period

A) PROTECTIVE MEMBRANE LAYER

[Stein & Stevels, 1964], [de Jong, 1967], [Kondo & Daimon, 1968], [Brown et al. 1985]

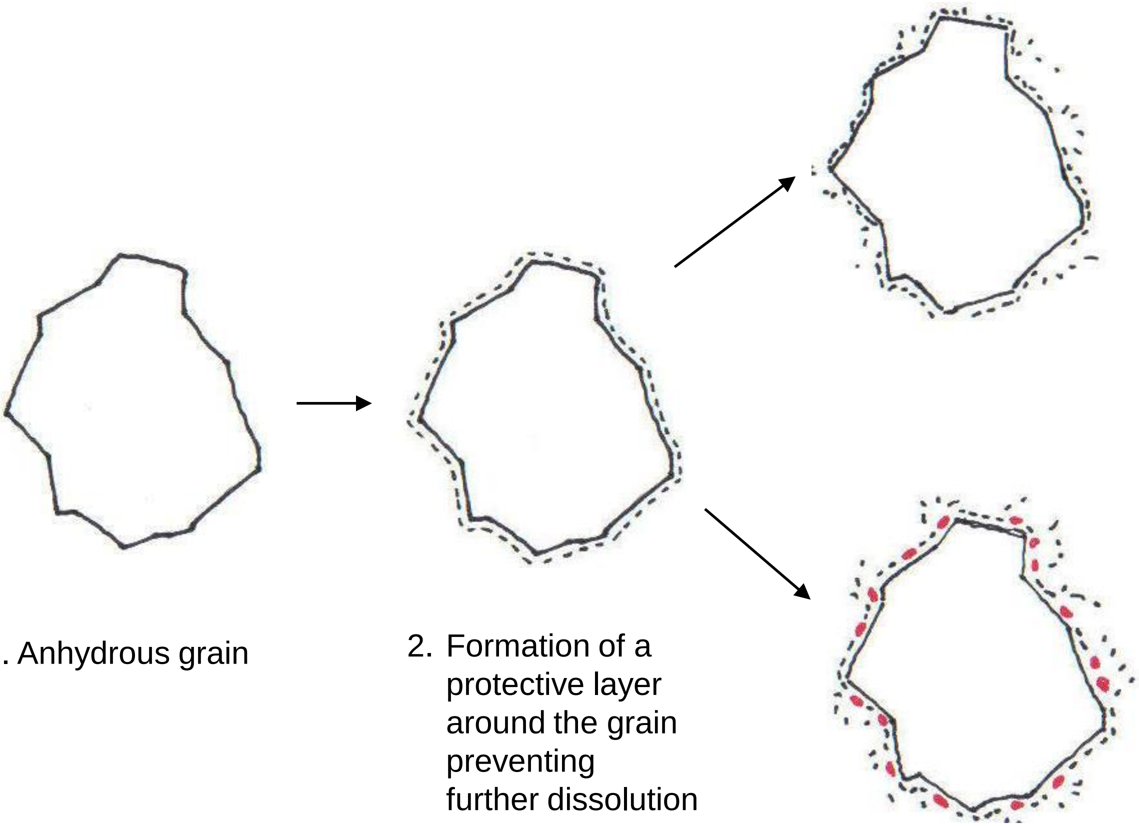

1. Anhydrous grain

2. Formation of a protective layer around the grain preventing further dissolution

3.a) Disruption of the protective layer by osmotic pressure due to the difference of ion concentration between the inner solution and the pore solution creating an osmotic pressure.

[Powers], [Double et al., 1980]

3.b) Disruption of the protective layer due to the nucleation and growth of more stable hydrates in the protective membrane

[Stein & Stevels, 1964]
[Gartner & Jennings, 1987]

Different theories about the induction period

B) NUCLEATION THEORY

[Fierens and Verhaegen, 1976],[Odler and Dorr, 1979],[Gauffinet et al., 1998]

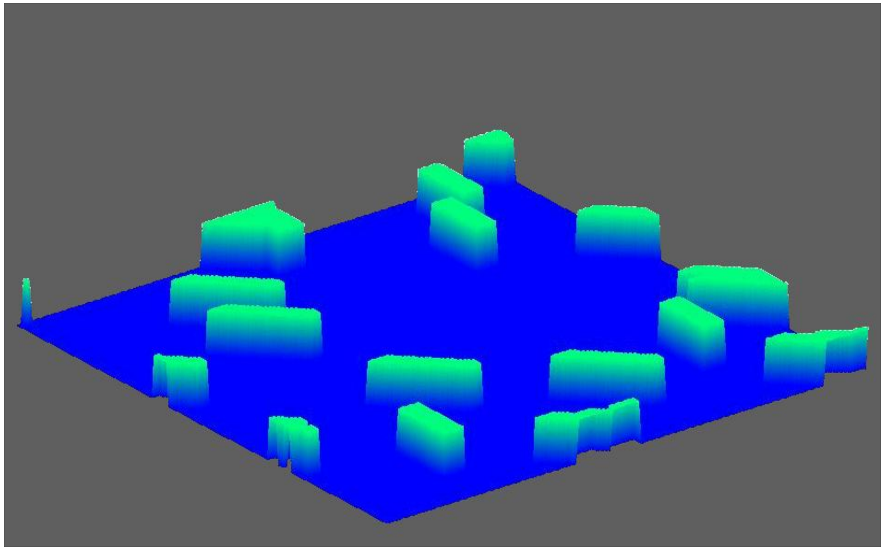

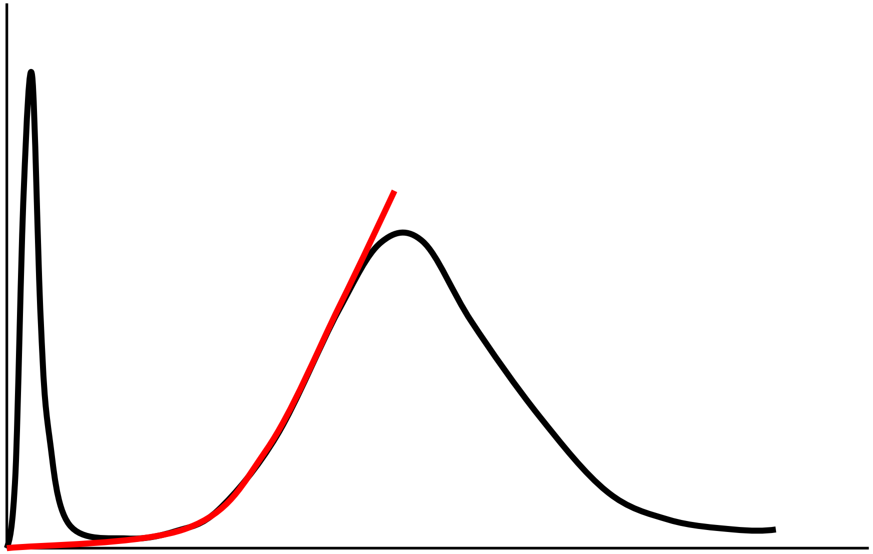

Formation of nuclei on surface controls early reaction of hydration. Growth of the nuclei is the rate limiting factor.

Is there an induction period ?

[Garrault et al., 2007]

From the point of view of geochemistry

To date, major findings show that dissolution of crystals preferentially occurs at specific surface sites that are characterised as having “excess surface energy”. This suggests that dissolution is directly controlled by surface reactions at reactive sites. These sites include **defects, dislocations, twinning and grain boundaries**

[Hegleson et al., 1984], [Lasaga et al., 1986].

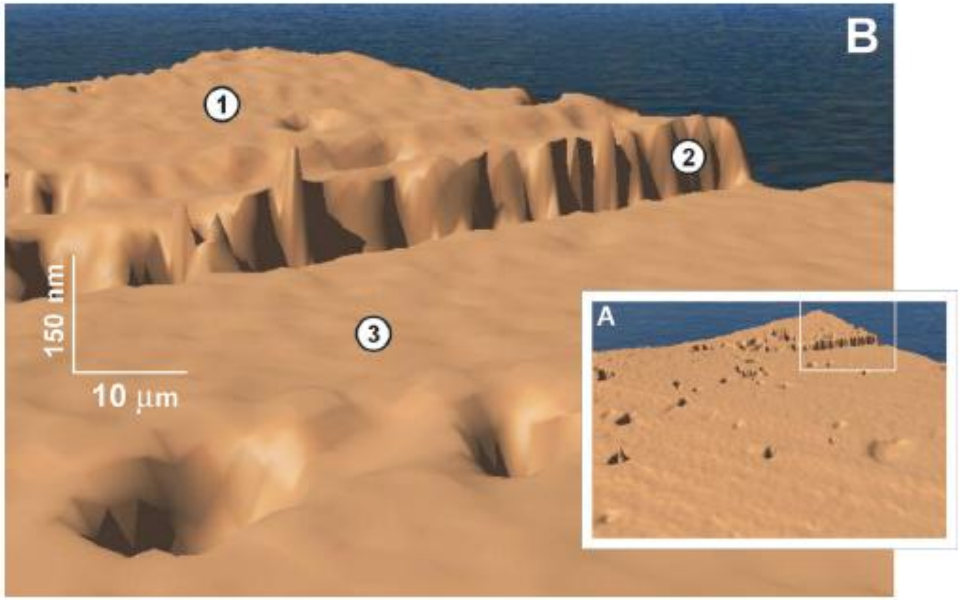

Fig. 1. (**A**) Vertical scanning interferometry scan of a dolomite cleavage showing both individual etch pits and the overall retreat of the mineral surface at pH 3 and 25°C after a 1-hour run duration (*21*). (**B**) Enlargement of the rectangular area in (A). Point 1 shows where the reference glue was removed, point 2 shows global dissolution, and point 3 shows the reactive surface area with etch pits.

[Lasaga and Lüttge, 2001]

Mechanisms of dissolution as a function of undersaturation

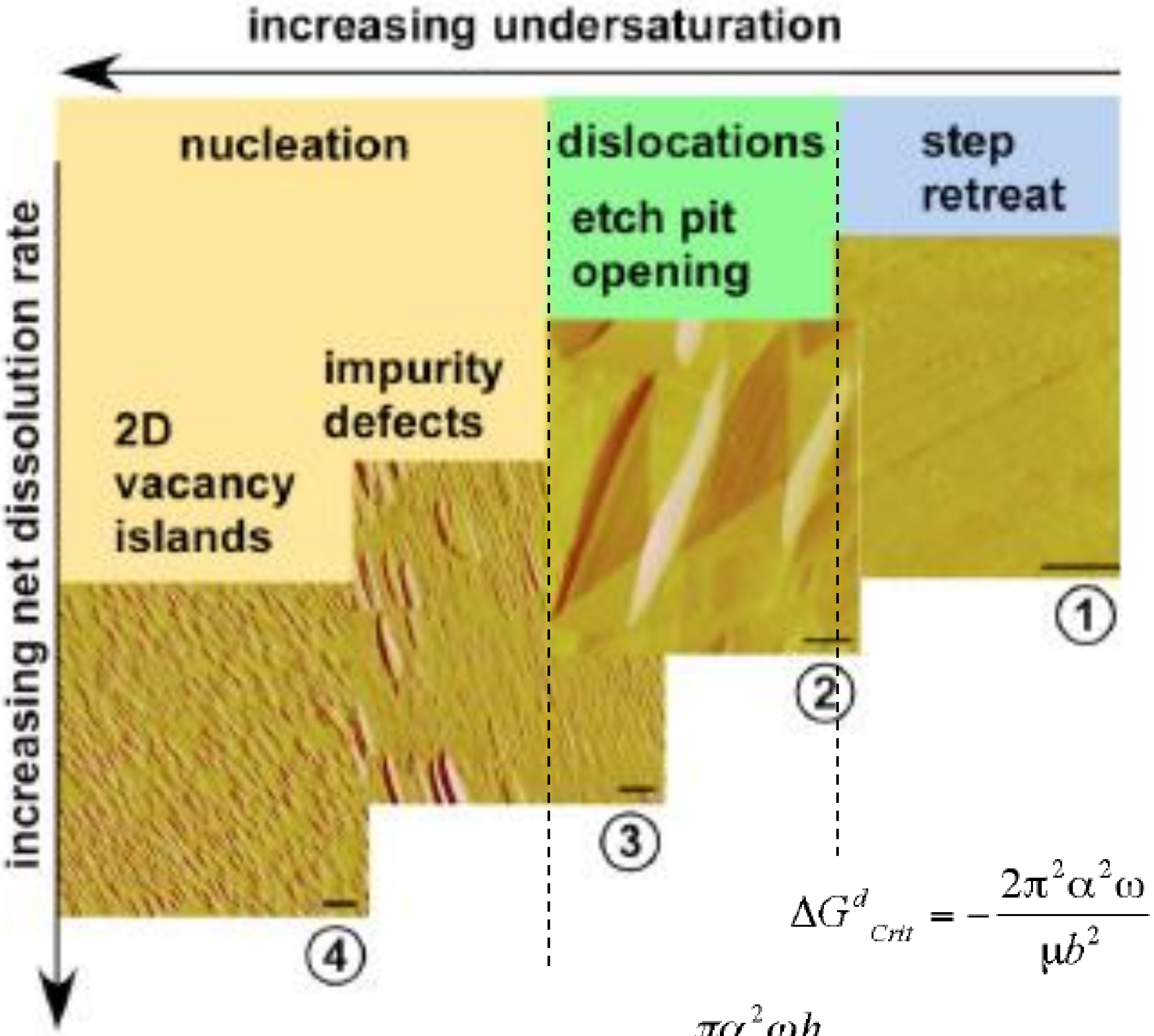

$$\Delta G^{d}{}_{Crit} = -\frac{2\pi^2\alpha^2\omega}{\mu b^2}$$

$$\Delta G^{n}{}_{Crit} = -\frac{\pi\alpha^2\omega h}{\mathbf{k}T\ln\Omega}$$

[Dove et al., 2007]

Evolution of the two energy barriers as a function of the undersaturation

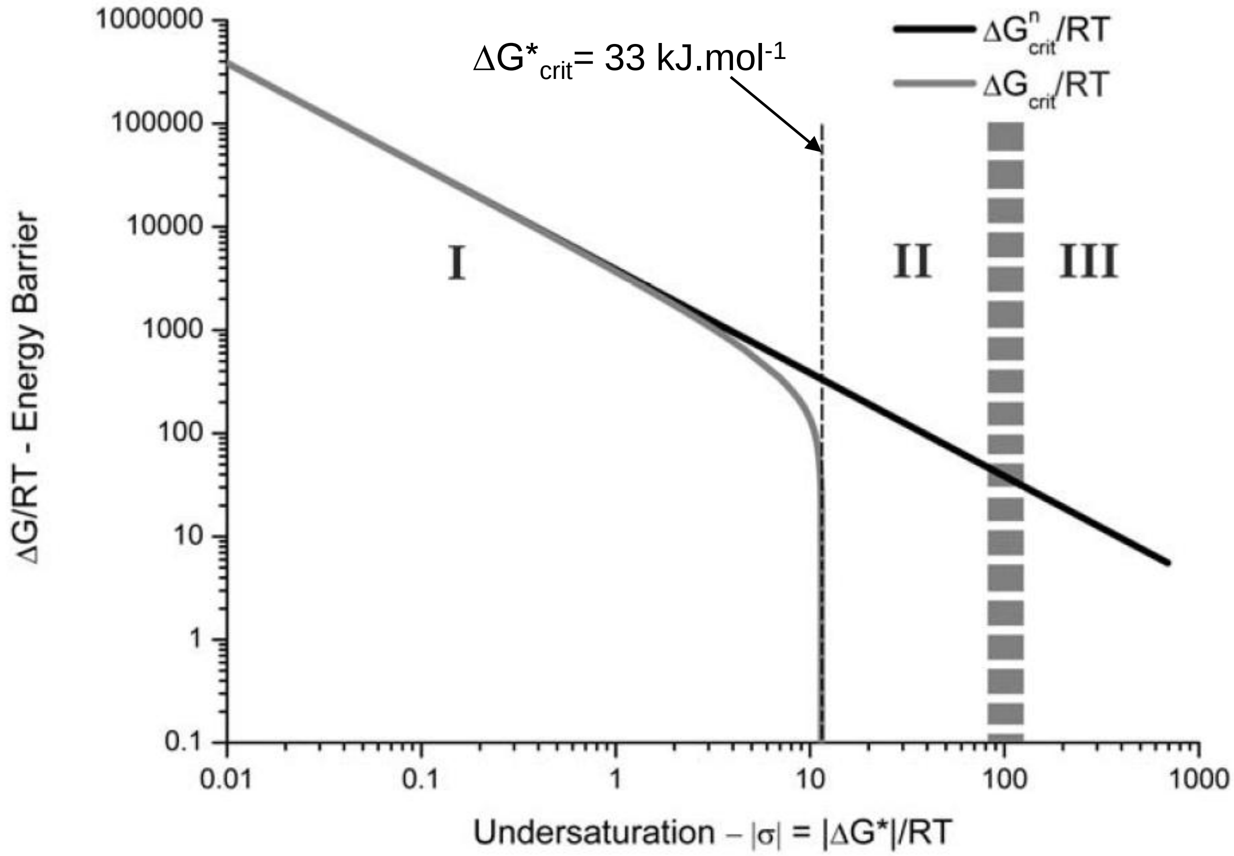

I: Regime of dissolution controlled by step retreat

II: Regime of dissolution controlled by etch pit forming at dislocation

III: Regime of dissolution controlled by 2D vacancy islands nucleation

Calculation made for albite with values taken from [Burch et al., 1993]

Comparison of the full dissolution theory with experimental data.

ΔG^*_{crit}= 33 kJ.mol^{-1} corresponding to an undersaturation of -11

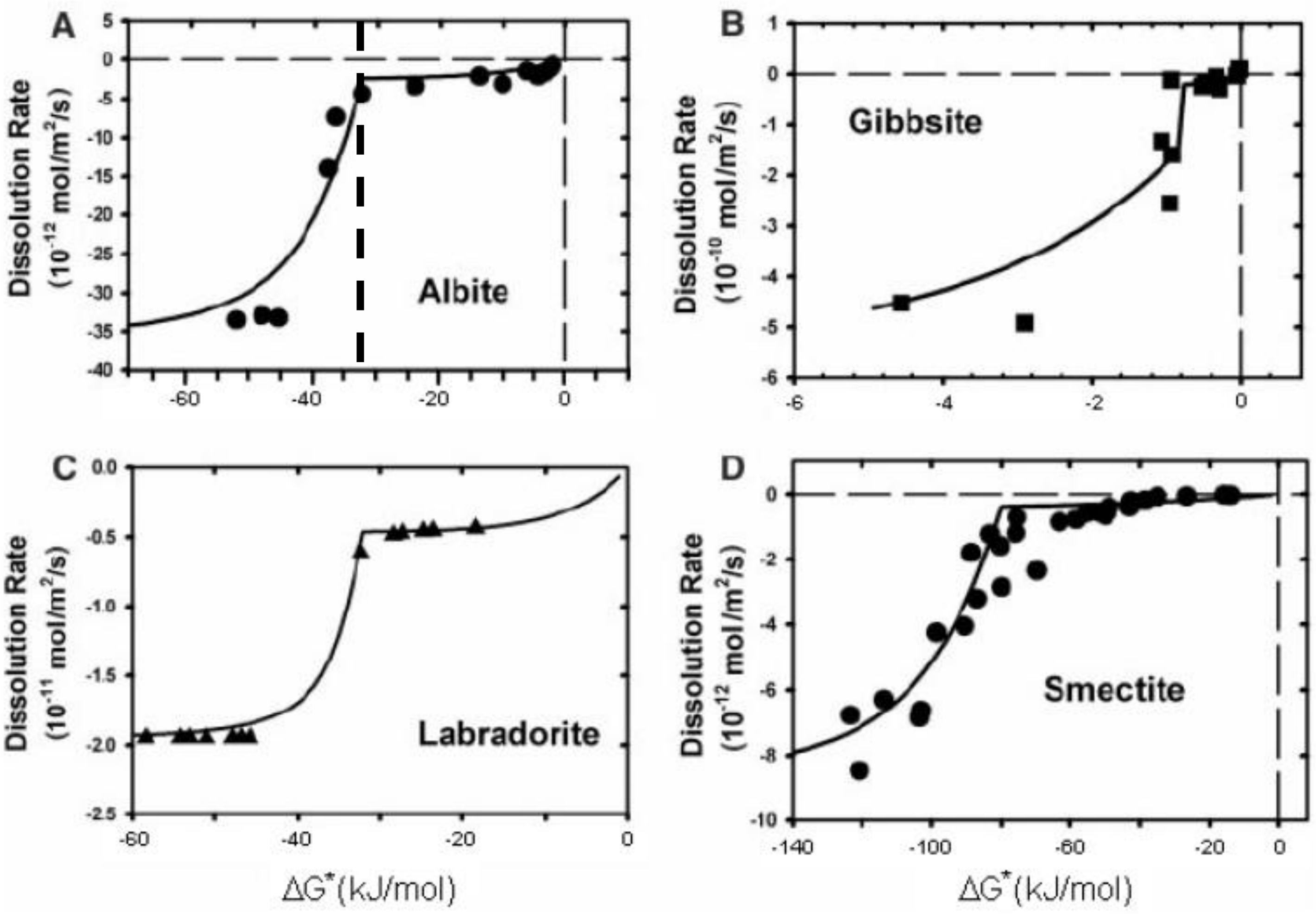

(A) Albite at pH 8.8 and 80°C. (B) Gibbsite at ph 3 and 80°C. (C) Labradorite at pH 3 and 25°C. (D) Smectite at pH 3 and 80°C

(Adapted from [Lasaga and Lüttge, 2001])

Albite dissolution experiments at 80°C and pH 0f 8.8

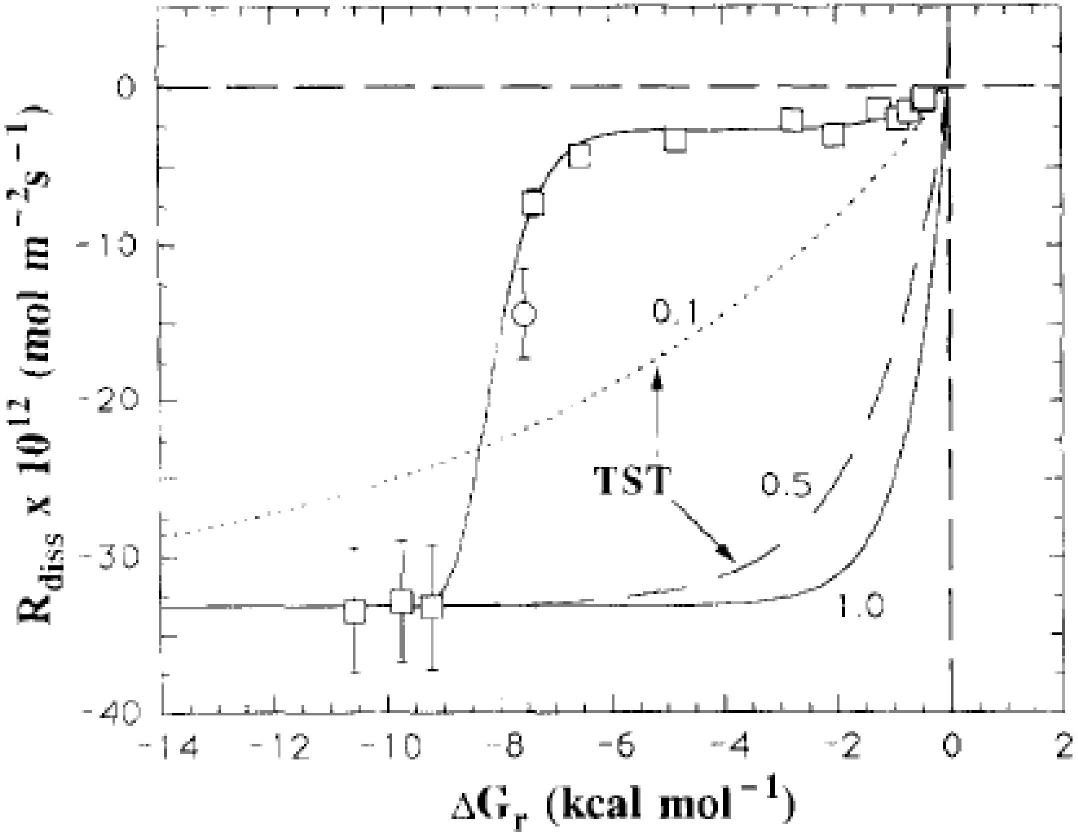

TST: $f(\Delta G_r) = [1 - \exp(n\Delta G_r/RT)]$

[Burch et al., 1993]

AFm measurement on **CALCITE**: Effect of the undersaturation coefficient

Decrease of the ionic concentration →

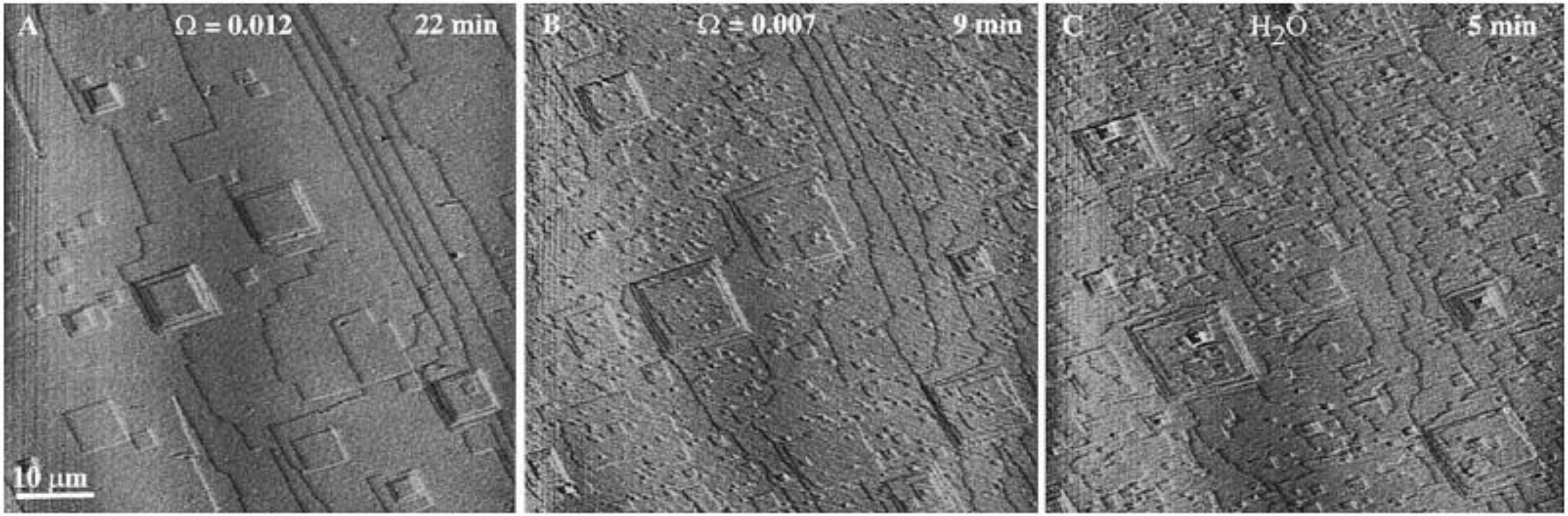

Fig. 4. In situ AFM images of a dissolving $\{10\bar{1}4\}$ surface showing the abrupt leap in pit density when the saturation index decreases from (A) $\Omega = 0.012$ to (B) $\Omega = 0.007$ and the resemblance of the surface morphologies at (B) $\Omega = 0.007$ and in (C) distilled, deionized water.

[Teng, 2004]

SEM: Anhydrous C_3S

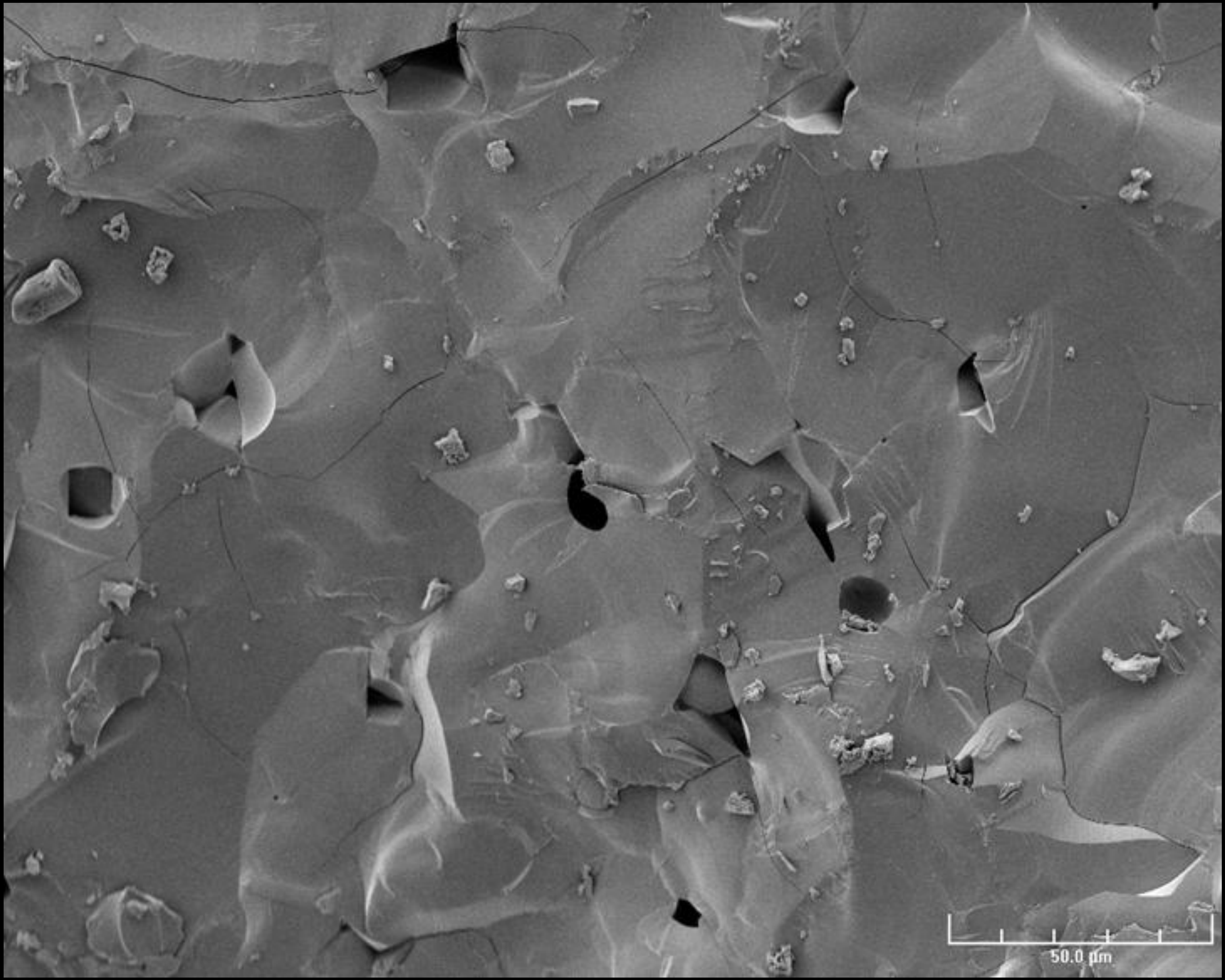

SEM: Anhydrous C_3S

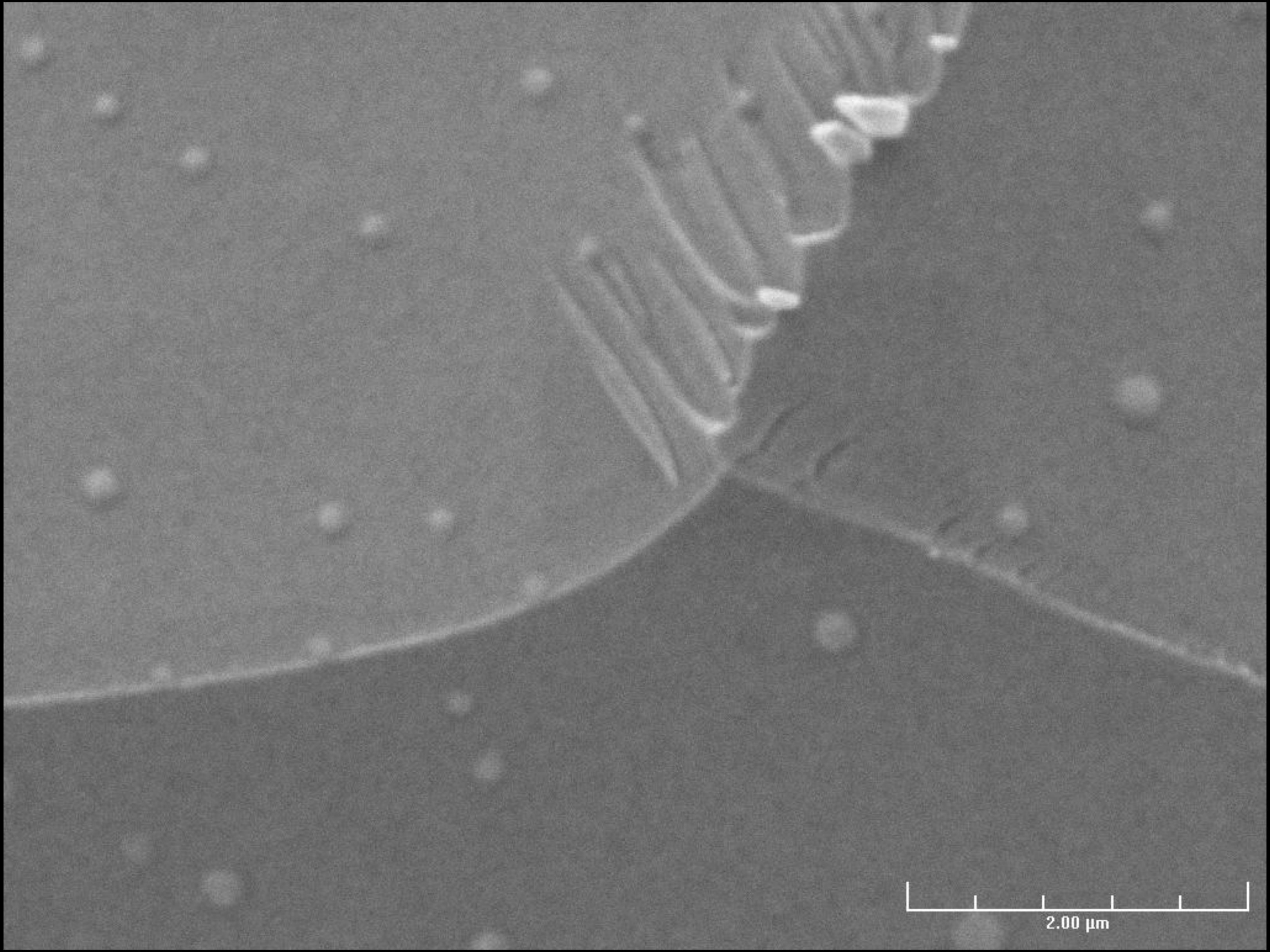

SEM: C_3S in water for 2 minutes (very diluted system)

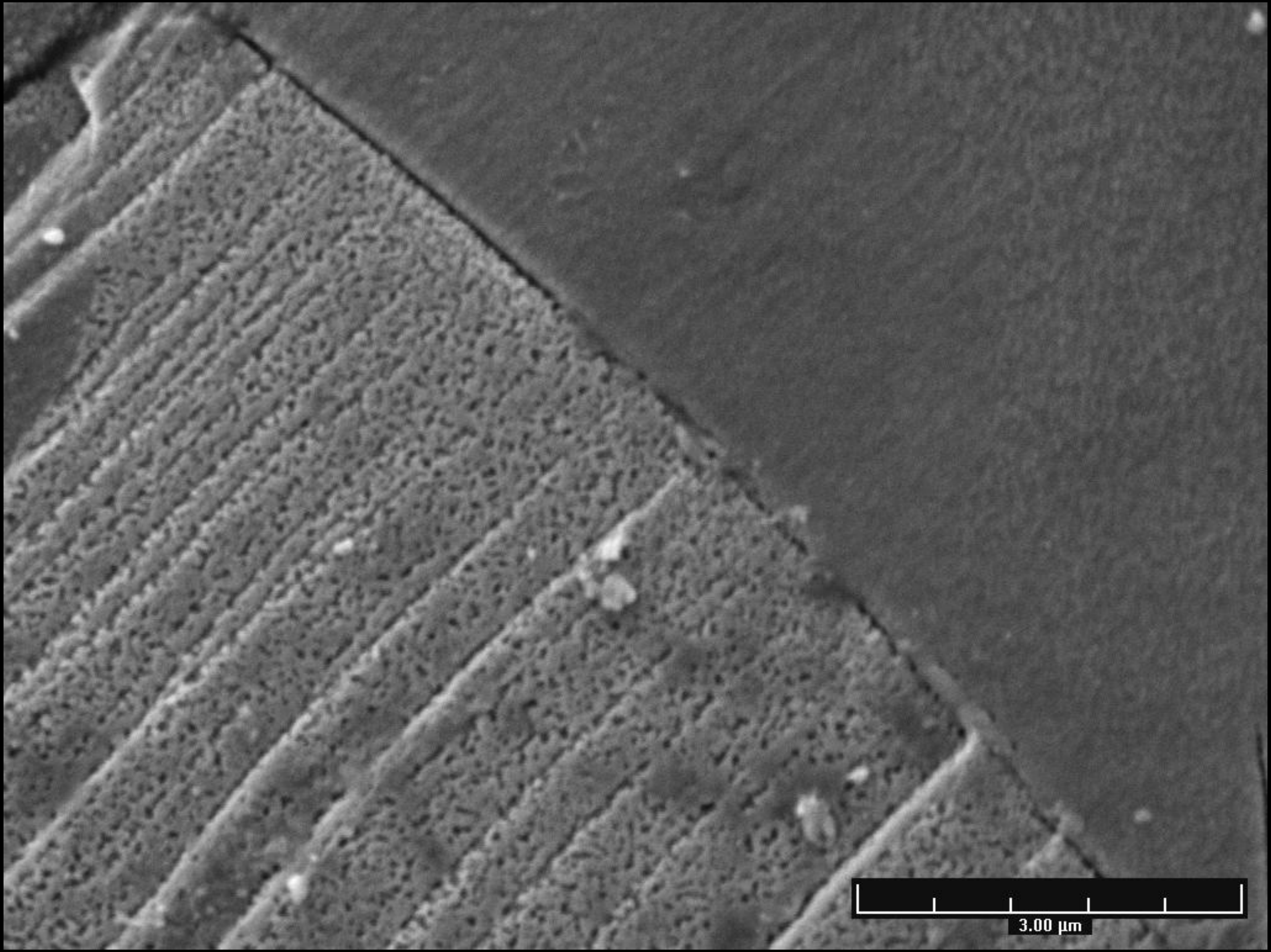

SEM: C_3S in water for 2 minutes (very diluted system)

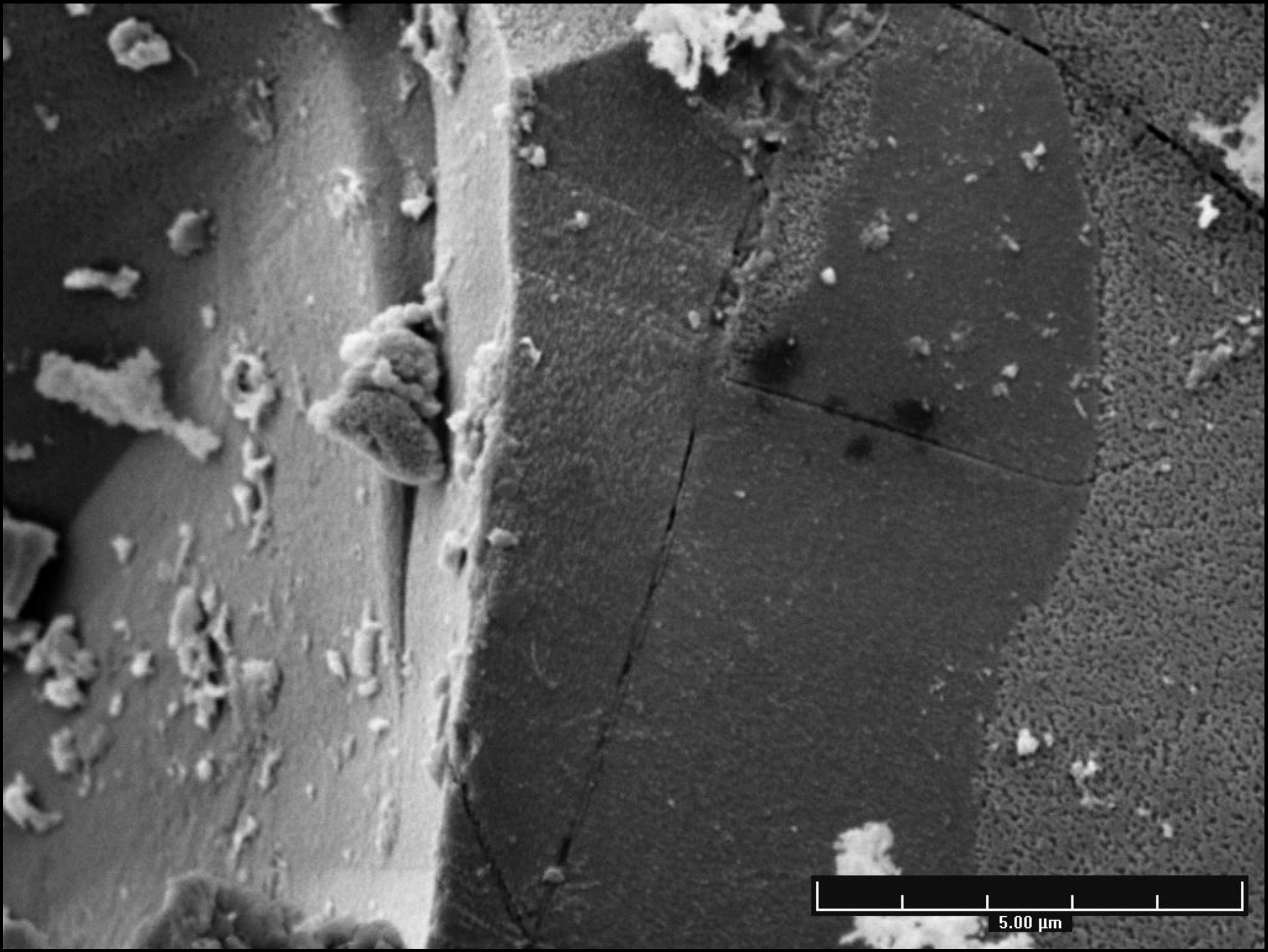

SEM: C_3S in water for 30 minutes

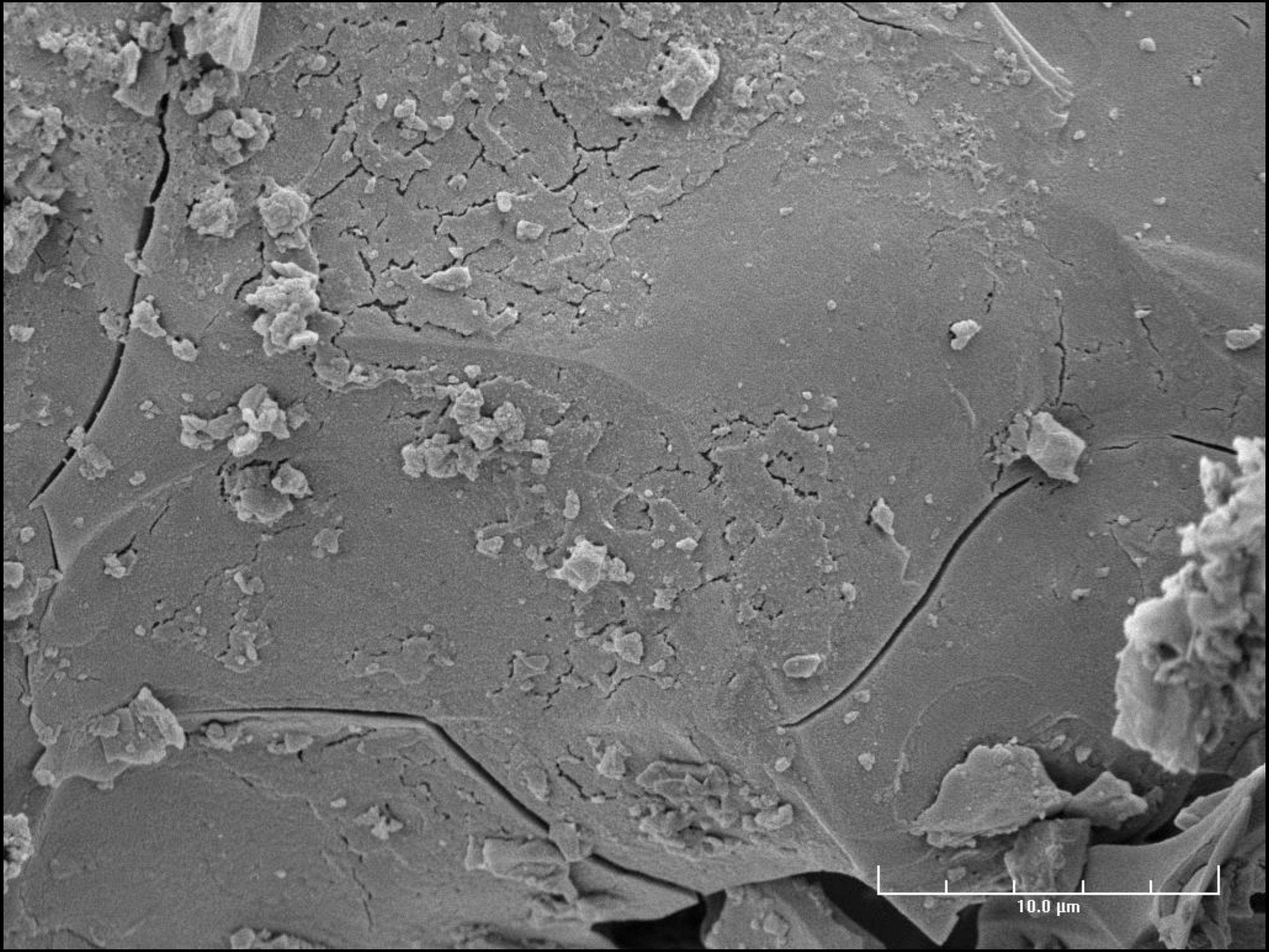

SEM: C_3S in water for 30 minutes

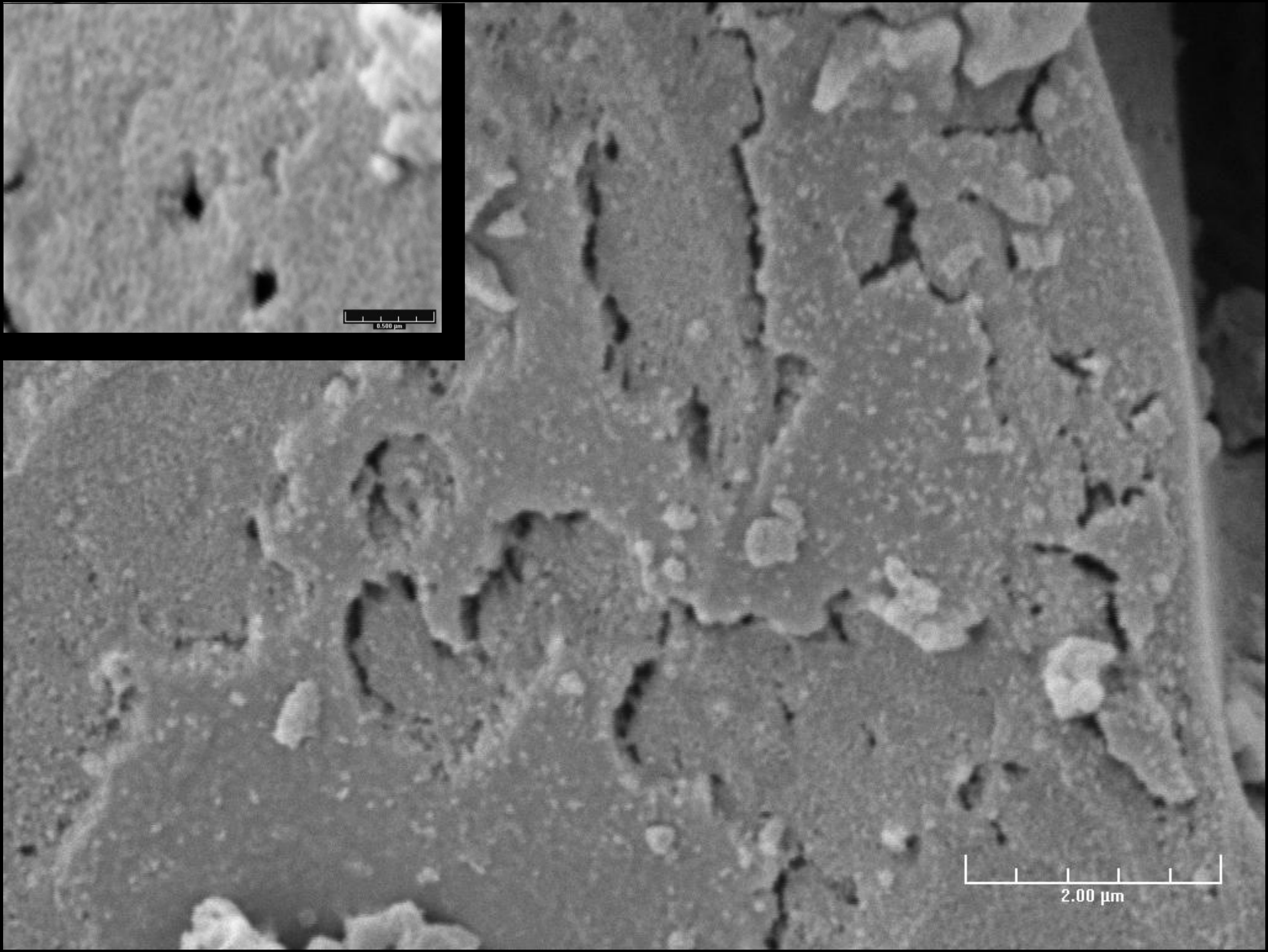

SEM: C_3S in saturated lime solution for 2 minutes

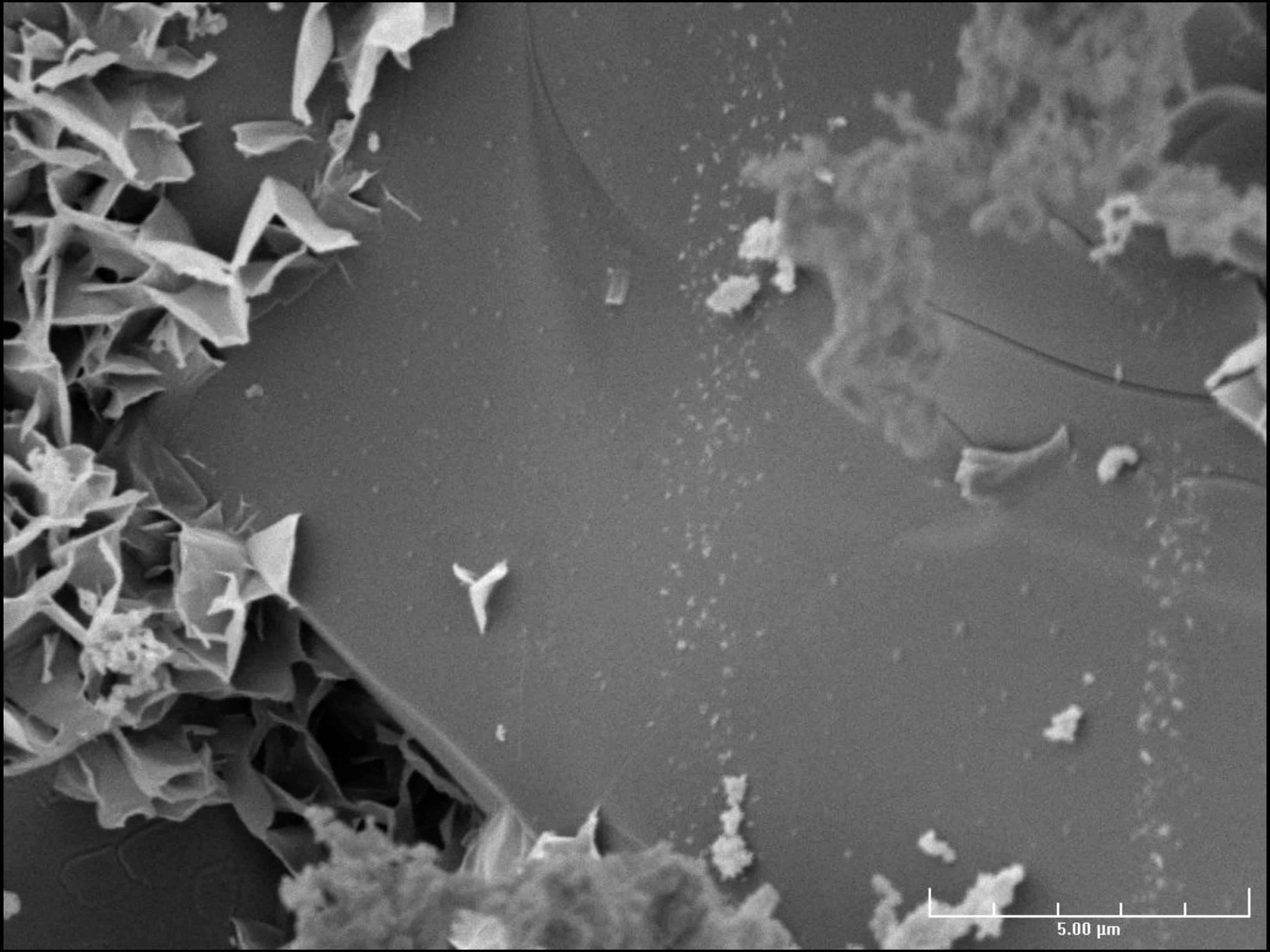

SEM: C_3S in saturated lime solution for 2 minutes

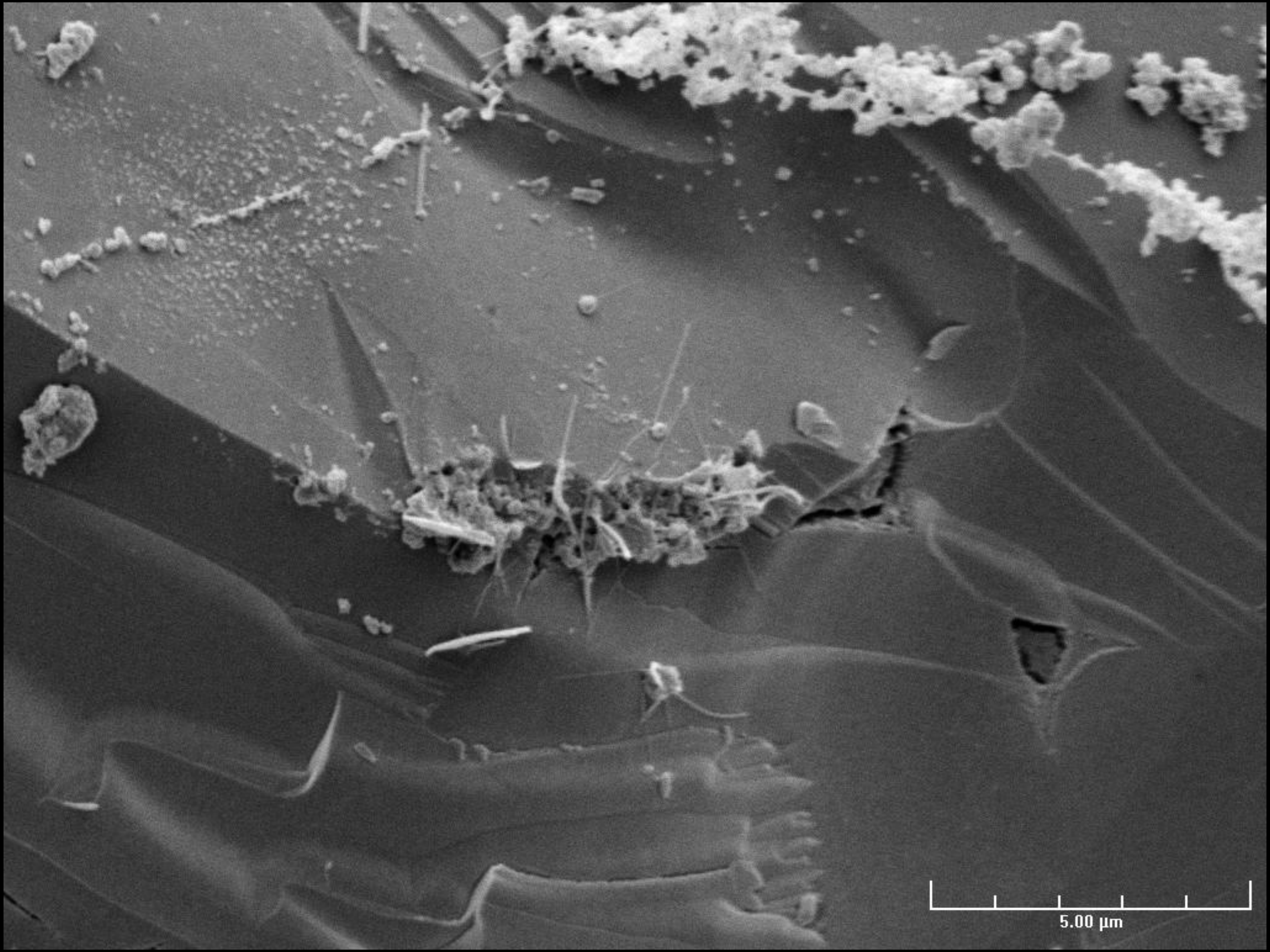

SEM: C_3S in saturated lime solution for 30 minutes

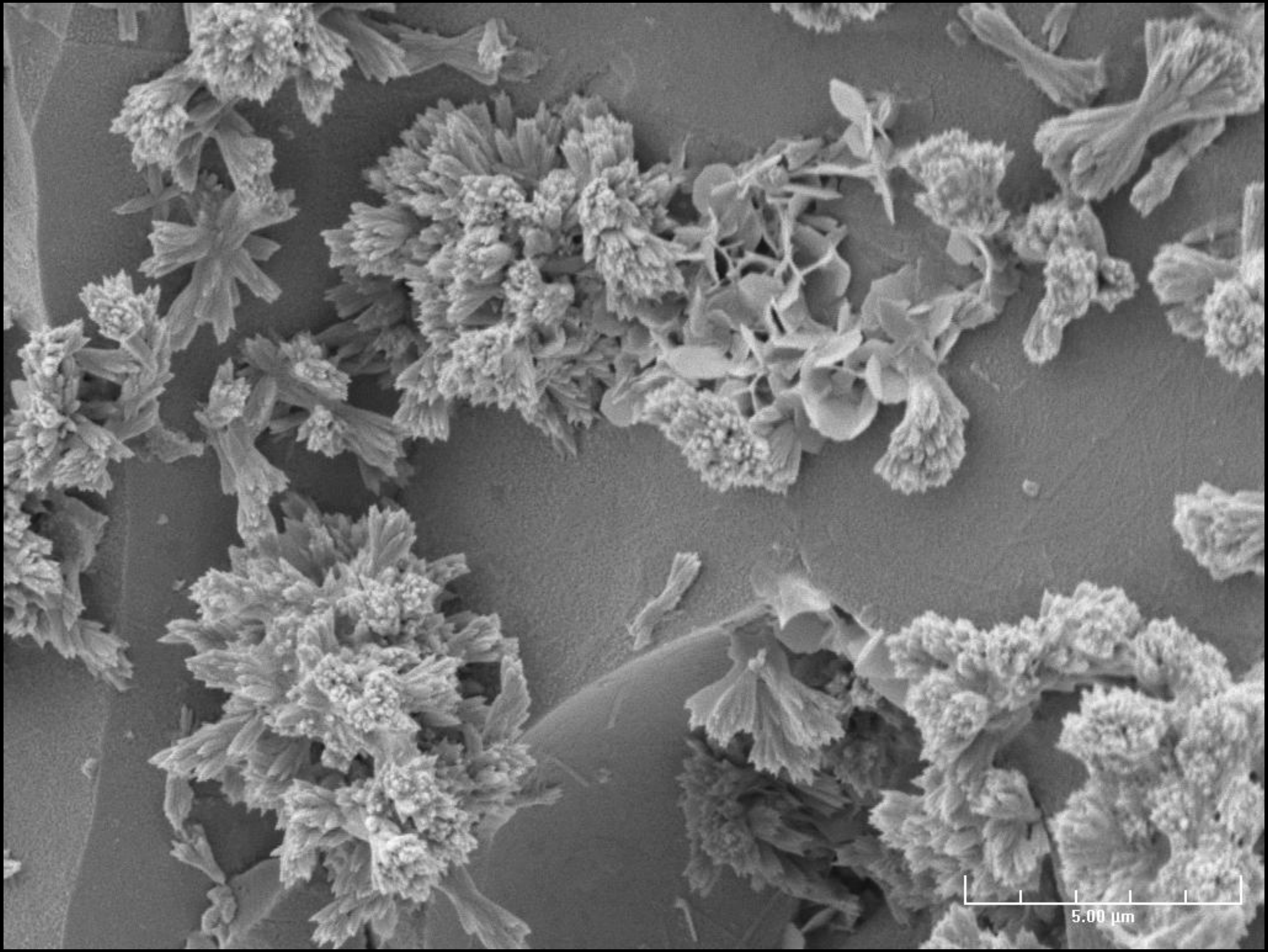

SEM: C_3S in saturated lime solution for 30 minutes

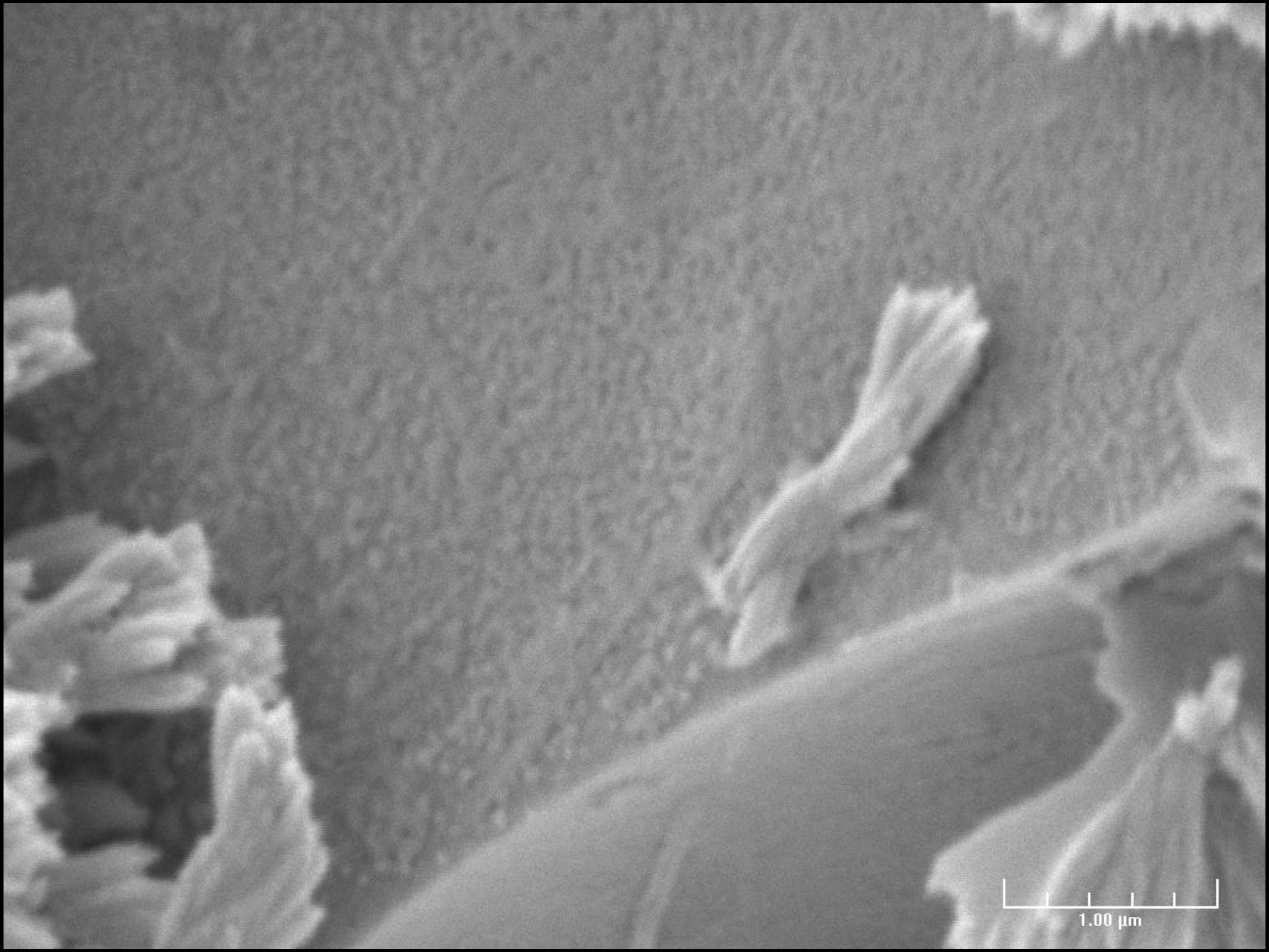

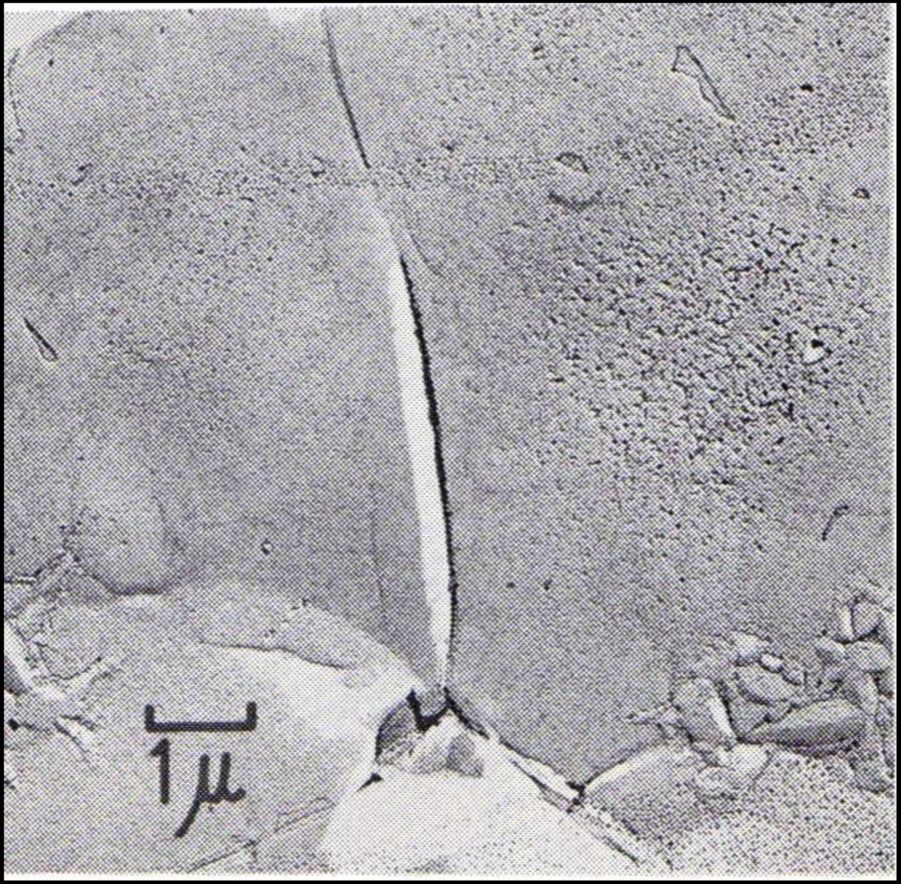

Change of crystal surfaces after 1 minute in etchant

Specimen: C_3S_{ss} with 1.1 wt % Cr_2O_3

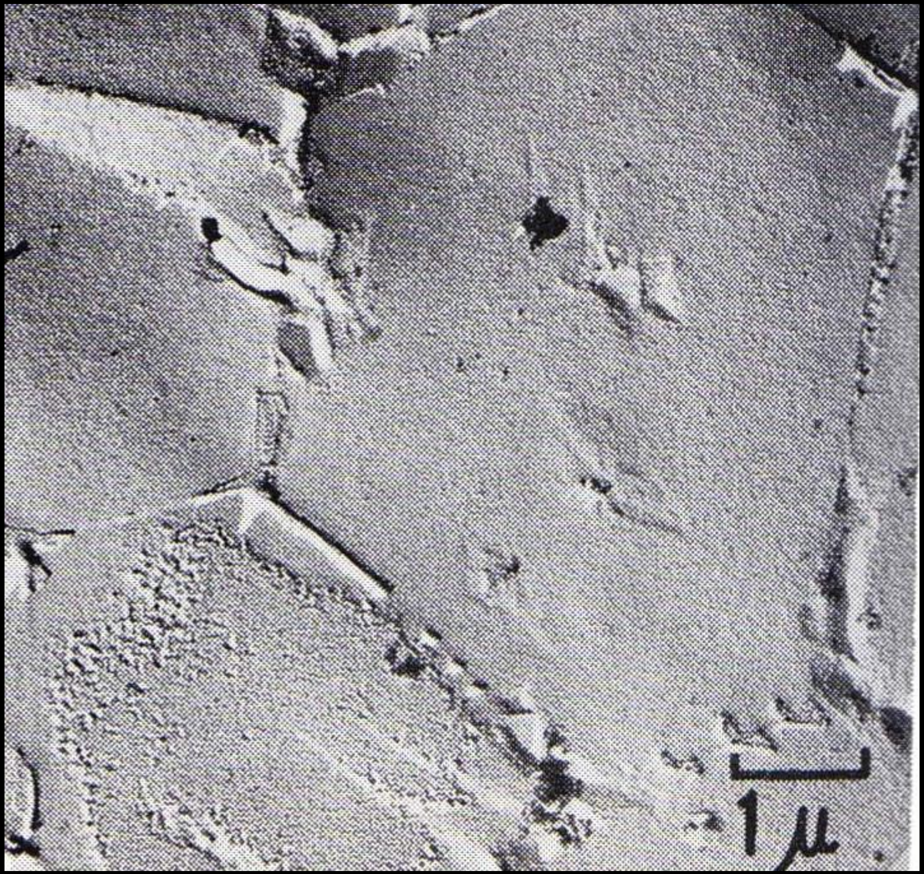

Change of crystal surfaces after 3 minutes in etchant

Etchant : 0.4% HF with 0.6% HNO_3 in ethyl alcohol

[Sakurai et al., 1968]

High-resolution SEM micrographs of hydrated C_3S surface

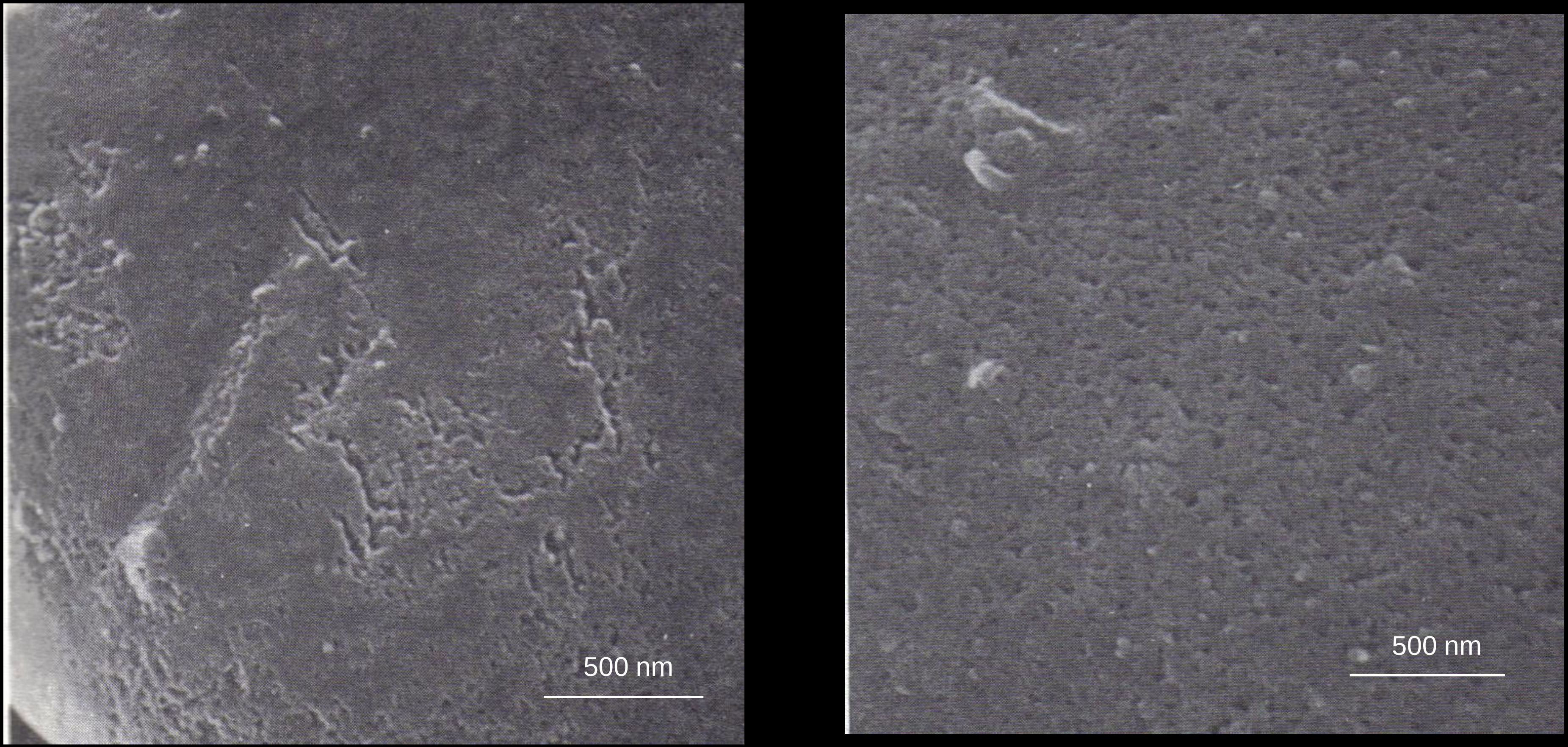

5 min

10 min

W/C = 1

[Ménétrier et al., 1979]

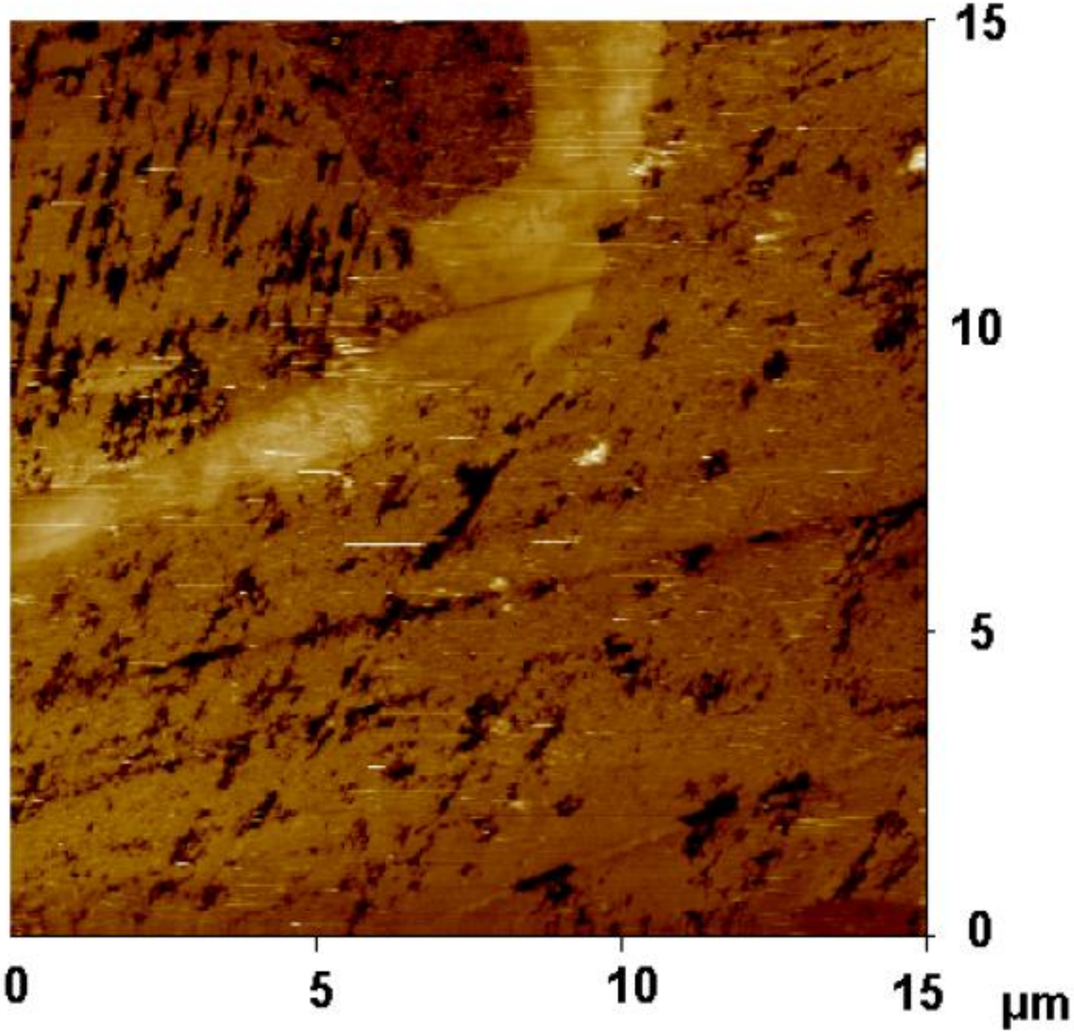

AFM image of a surface of alite hydrated for 5 hours in a saturated lime solution.

[Garrault et al., 1998]

Effect of annealing on alite of narrow particle size distribution

First dissolution peak

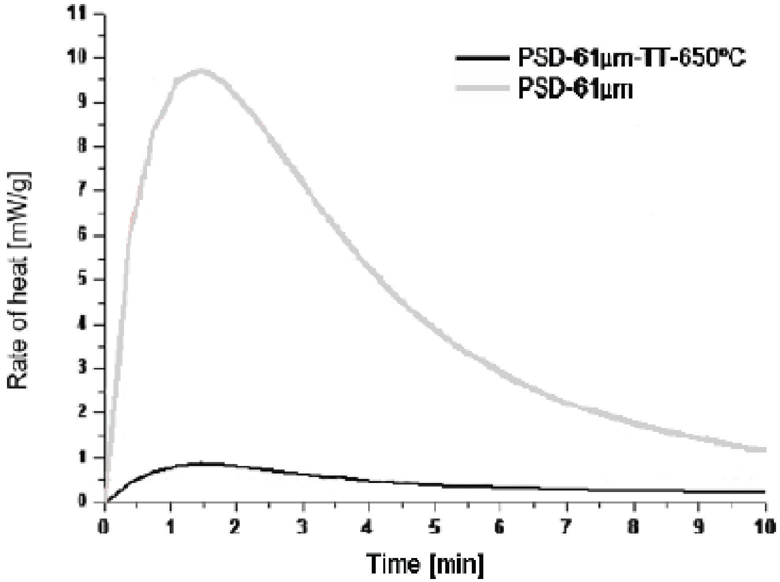

Normal calorimetry curves

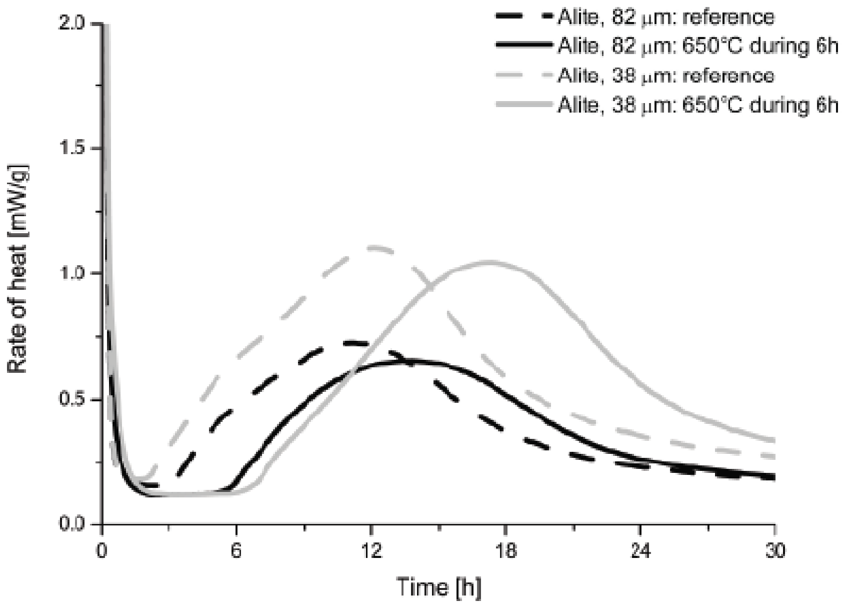

Proposed mechanism: Microstructural development at early age

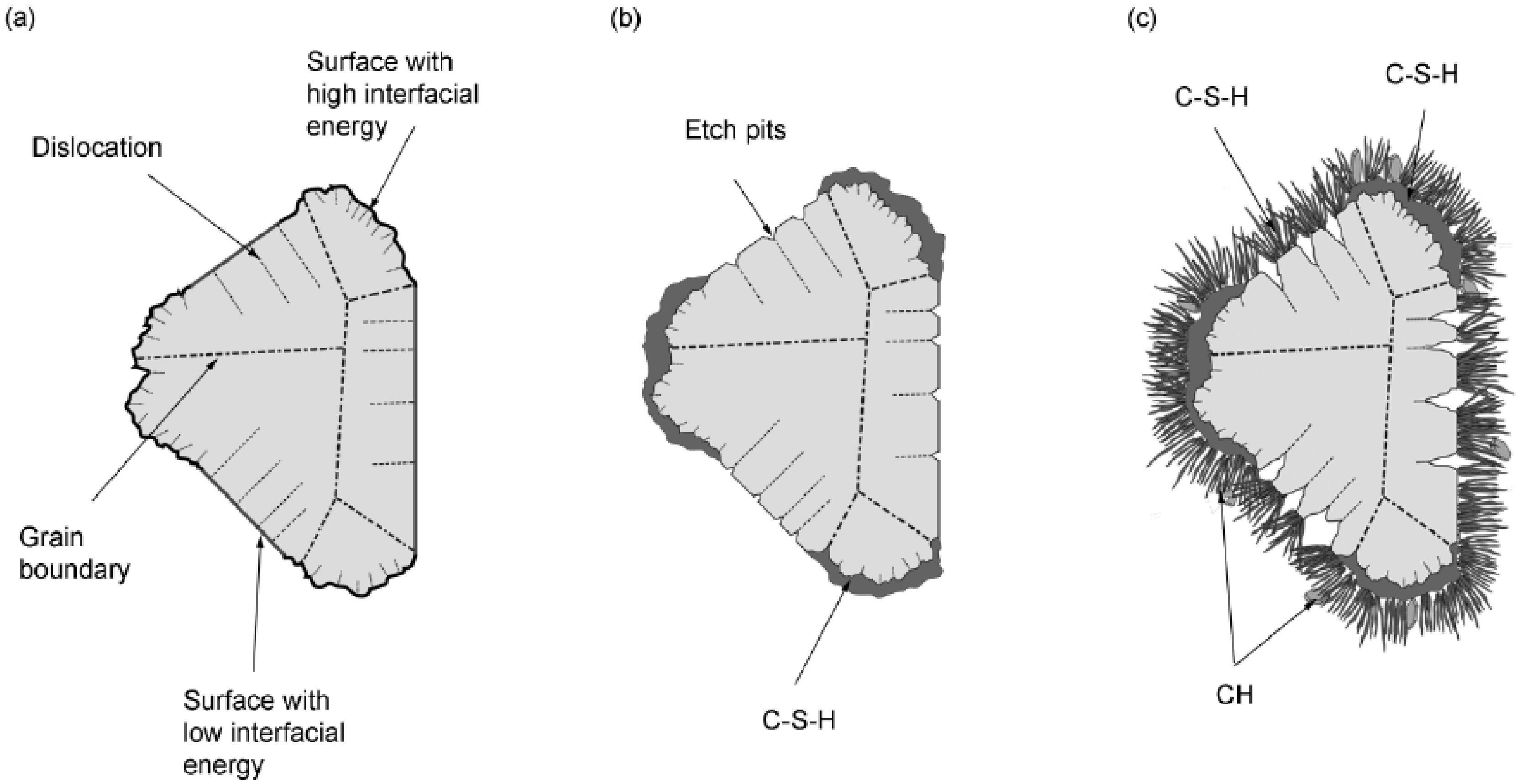

Proposed mechanism: Evolution of the rate of dissolution

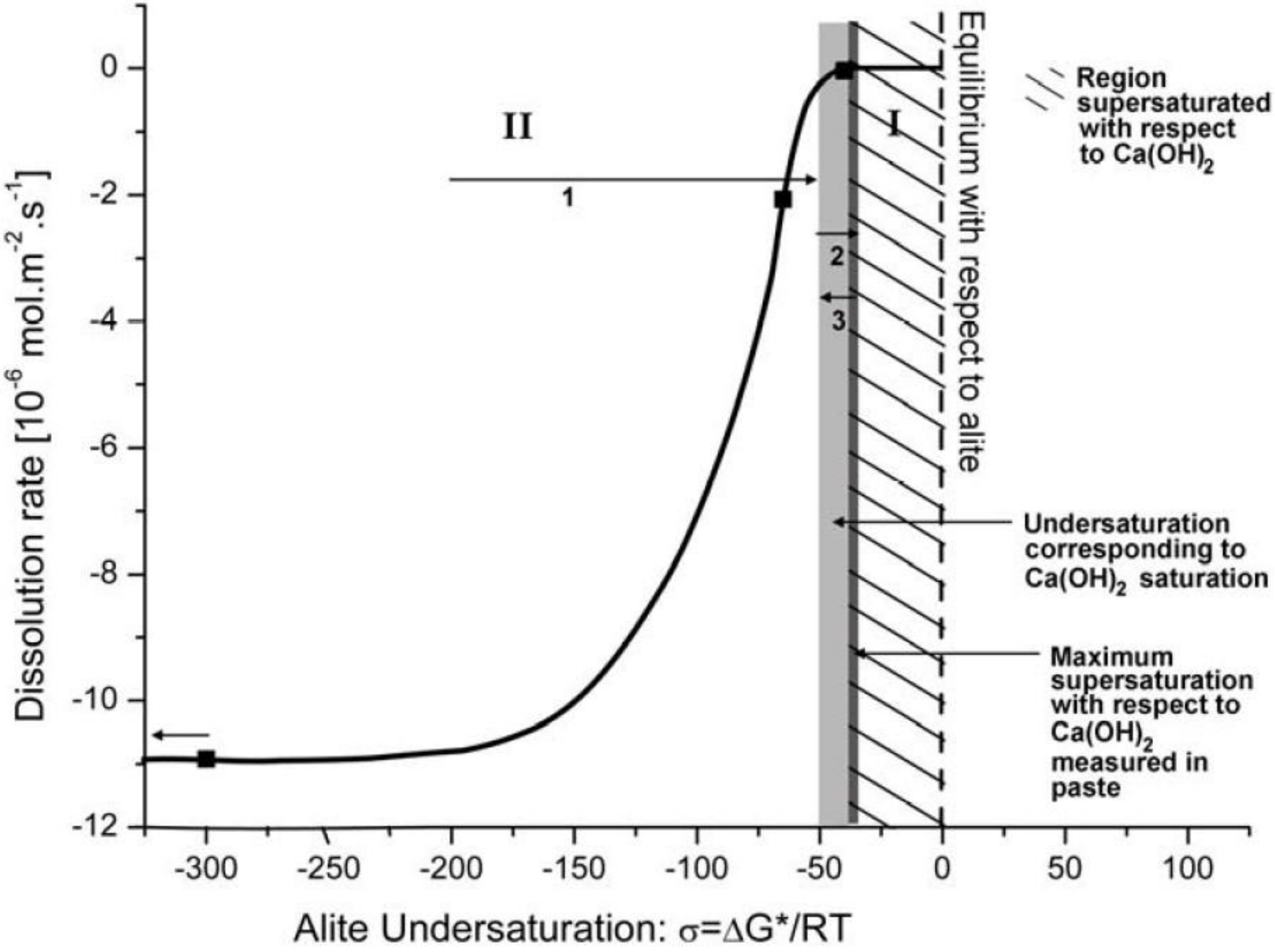

Experimental data points for dissolution rate from [Damidot et al., 2008]

Modelling of early age kinetics

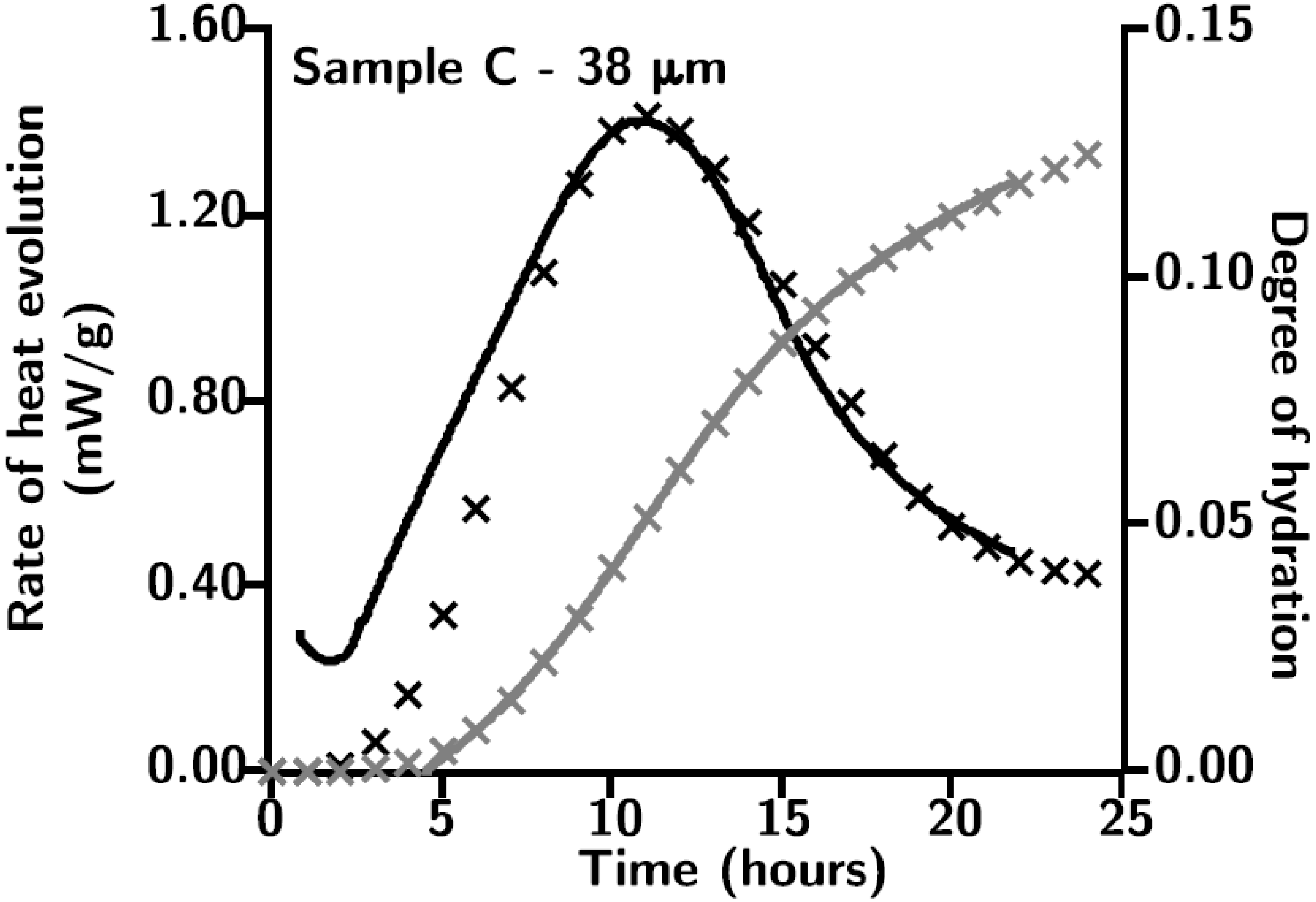

[Bishnoi and Scrivener, submitted]

Modelling of early age kinetics

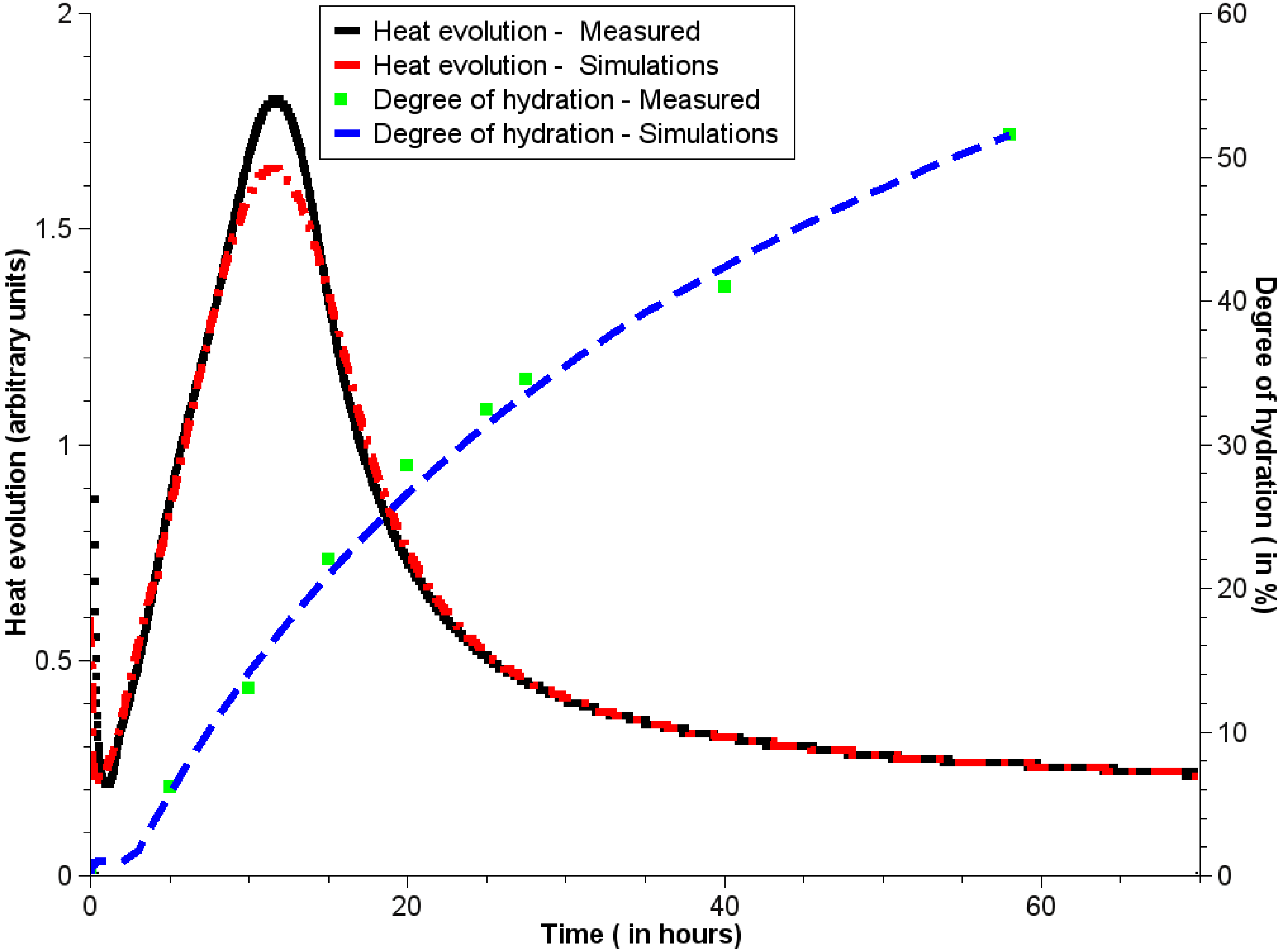

[Kumar, 2009]

Modelling of early age kinetics

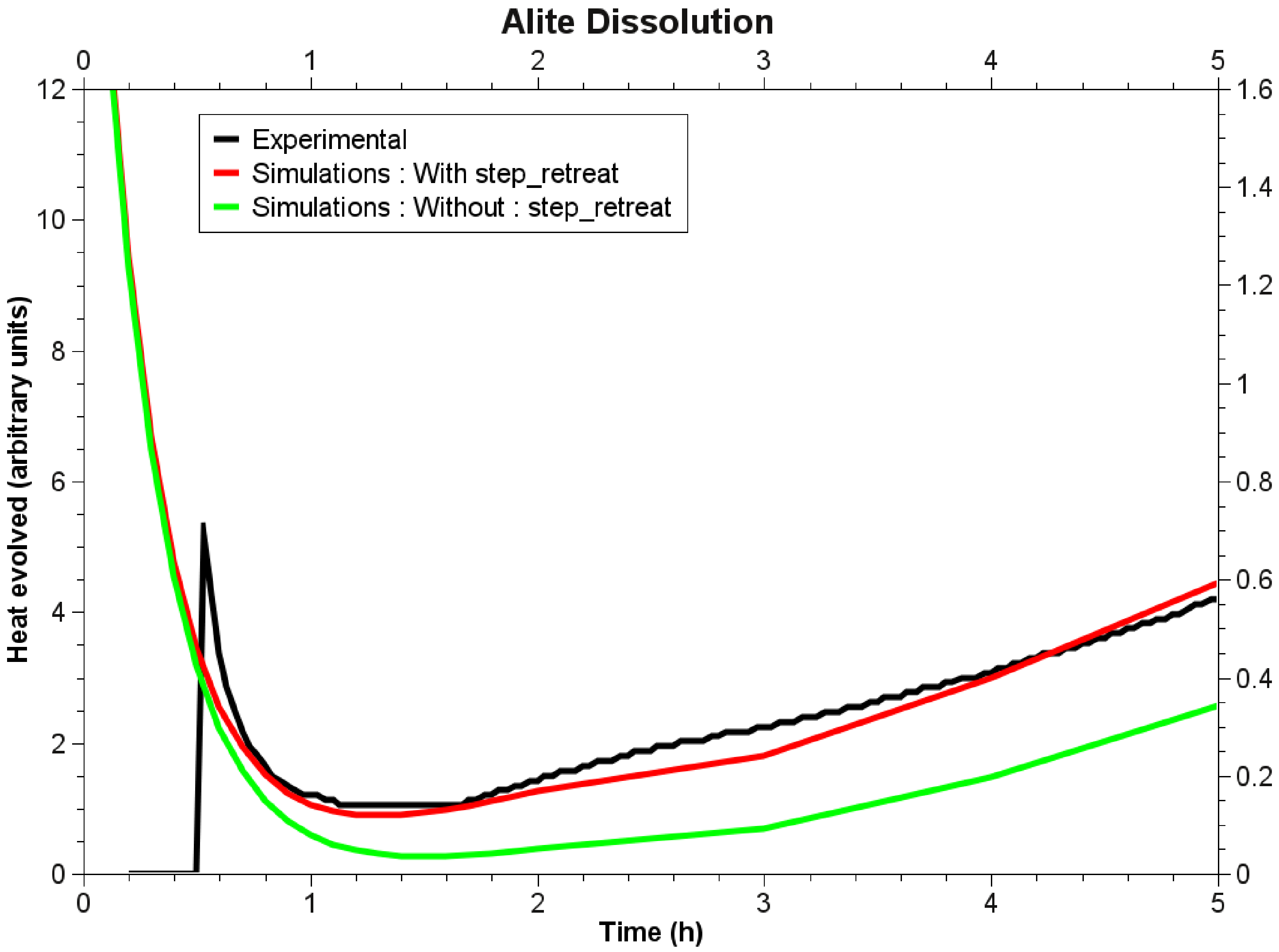

[Kumar, 2009]

Conclusions

- Strong dependence of the rate of dissolution with the saturation state of the solution

- Duration of the induction period affected by the density of defects

- Observations of etch pits

- Possibility to model properly the early hydration using µic.